FULL PAPER *Internal Medicine*

Feasibility of radial and circumferential strain analysis using 2D speckle tracking echocardiography in cats

Hiroshi TAKANO[1,2)]*, Tomomi ISOGAI[1)], Takuma AOKI[1)], Yoshito WAKAO[1)] and Yoko FUJII[1)]

[1)]*Department of Surgery 1, School of Veterinary Medicine, Azabu University, 1–17–71 Fuchinobe, Chuo-ku, Sagamihara-shi, Kanagawa 252-5201, Japan*
[2)]*Research Fellow of the Japan Society for the Promotion of Science, 5–3–1 Kojimachi, Chiyoda-ku, Tokyo 102-0083, Japan*

(Received 14 May 2013/Accepted 19 October 2014/Published online in J-STAGE 6 November 2014)

ABSTRACT. The purpose of the present study is to investigate the feasibility of strain analysis using speckle tracking echocardiography (STE) in cats and to evaluate STE variables in cats with hypertrophic cardiomyopathy (HCM). Sixteen clinically healthy cats and 17 cats with HCM were used. Radial and circumferential strain and strain rate variables in healthy cats were measured using STE to assess the feasibility. Comparisons of global strain and strain variables between healthy cats and cats with HCM were performed. Segmental assessments of left ventricle (LV) wall for strain and strain rate variables in cats with HCM were also performed. As a result, technically adequate images were obtained in 97.6% of the segments for STE analysis. Sedation using buprenorphine and acepromazine did not affect any global strain nor strain rate variable. In LV segments of cats with HCM, reduced segmental radial strain and strain rate variables had significantly related with segmental LV hypertrophy. It is concluded that STE analysis using short axis images of LV appeared to be clinically feasible in cats, having the possibility to be useful for detecting myocardial dysfunctions in cats with diseased heart.
KEY WORDS: feline hypertrophic cardiomyopathy, left ventricle

doi: 10.1292/jvms.13-0241; *J. Vet. Med. Sci.* 77(2): 193–201, 2015

Left ventricular concentric hypertrophy (LVH) is the most common pathologic condition of cardiac disease in cats. Hypertrophic cardiomyopathy (HCM) is a major underlying cause of LVH, but LVH has numerous secondary causes, such as systemic hypertension, hyperthyroidism, aortic stenosis and acromegaly [1, 6, 13, 17, 31].

The gold standard method of morphological evaluation for LVH in clinical practice is echocardiography. LVH is generally diagnosed when the left ventricular (LV) diastolic wall thickness is 6 mm or more [1]. However, LVH of all feline patients is reportedly not symmetric in some etiologies of LVH including HCM, systemic hypertension and hyperthyroidism [1, 6, 7, 13]. In a word, LVH patterns in cats show variety. Furthermore, in the early stage of pathological conditions, hypertrophy of ventricular wall may not be obvious. For these reasons, morphological abnormalities of LV wall could not be detected by evaluations using the standard echocardiogram including B- and M-mode.

To detect myocardial dysfunctions of left ventricle in its early stage, the availability of tissue Doppler imaging (TDI) has been assessed in cats [20, 21, 38, 43]. However, in TDI, feasible measurement sites are limited, because of angle dependence. Speckle tracking echocardiography (STE) is an approach designed to assess myocardial functions of the ventricle and atrium using speckle patterns of myocardial tissue in a B-mode image [4, 5, 14, 37]. The capabilities of segmental and multi-directional assessments of myocardial functions using STE could possibly serve as one of the useful tools in evaluations of local myocardial functions and early detection of myocardial dysfunctions.

However, since an analysis of STE strongly relies on the resolution of a B-mode image, and since a high heart rate in cats would influence the quality of images, the feasibility of STE should be evaluated first. The aims of this study are: (1) to assess the feasibility of application of STE to cats by using clinically healthy individuals and (2) to evaluate STE variables in cats with HCM.

MATERIALS AND METHODS

Study population: Sixteen clinically healthy cats (12 domestic shorthairs, 1 Abyssinian, 1 Norwegian Forest Cat and 2 Russian Blues) were used in the present study as a control group. They were considered clinically normal when no evidence of cardiopulmonary and systemic disease that might influence their cardiac functions was noticed, based on a physical examination, an electrocardiogram (standard limb lead), thoracic radiography and echocardiography, a complete blood count, a serum biochemical test, a urine specific gravity of>1.035 and a systemic blood pressure of <170 mmHg in systole.

The HCM group consisted of 17 client-owned cats with HCM diagnosed at the Azabu University Veterinary Teaching Hospital (8 American shorthairs, 3 Domestic shorthairs, 3 Scottish Fold, 1 Persian, 1 Chinchilla and 1 Russian Blue). They were clinically diagnosed as HCM when: 1) the interventricular septum and/or LV free-wall thickness during end-diastoles (IVSd and LVFWd) were greater than 6 mm,

*CORRESPONDENCE TO: TAKANO, H., Japan Animal Specialty Medical Institute Inc. (JASMINE), 2–7–3 Nakagawa, Tuduki, Yokohama, Kanagawa 024-0001, Japan. e-mail: h.takano@cardiovets.jp

and the LV end-diastolic internal diameter (LVIDd) was less than 18 mm by M-mode imaging of the left ventricular short-axis obtained from the right parasternal view [1]. 2) Values of blood nitrogen urea and creatinine fell within the reference range in serum biochemical testing or they did not exhibit systemic hypertension, and 3) hyperthyroidism was excluded on the basis of clinical signs and biochemistry, including serum T4 and hepatic enzyme concentrations. When a patient was younger than 4 years, hyperthyroidism was automatically excluded [8, 25]. HCM with a dynamic left ventricular outflow tract obstruction (LVOTO) was included in the present study. LVOTO was defined as a disturbed flow across the left ventricular outflow tract (LVOT) with an estimated pressure gradient greater than 30 mmHg concurrent with a late systolic acceleration [1, 27].

Systemic Arterial Blood Pressure Measurement: Systemic arterial blood pressure was measured indirectly on the tail or limb at a quiet and isolated place by the Doppler method as previously described using an aneroid sphygmomanometer (Tycos TR-2 Hand Aneroid Sphygmomanometer, Welch Allyn, Tokyo, Japan) [9]. Mean values of consecutive and stable measurements were used for the analysis.

Echocardiographic examination: Echocardiographic examinations were performed by two examiners (YF and HT) using one ultrasound machine (Vivid 7 dimension, GE Medical System, Tokyo, Japan). Cats were restrained manually in lateral recumbency. ECG monitoring (lead II) with a clear R wave recognition was recorded simultaneously using the same ultrasound machine used for the healthy cats. A transducer with 10 MHz was used to acquire all images. Data from 3 cardiac cycles were averaged and used for statistical analysis. Off-line STE measurements for main analysis were obtained by the same examiner (HT), and those for analysis of interobserver variabilities were by another (TI).

B-, M- and Doppler mode echocardiography: LV short-axis images at the chordae tendineae (Ct) level between the mitral valve and papillary muscle for M-mode measurements (IVSd, LVIDd, LVPWd and fractional shortening [FS]) and those at the aortic root level for B-mode measurements of the left atrium size (diameters of left atrial diameter [LAD] and aortic root, and the left atrium to aorta ratio [LA/Ao]) [2] were obtained on right lateral recumbency. Left atrial enlargement was defined as LA/Ao > 1.5 [43]. The segmental thickness of the interventricular septum below the aortic valve was measured at the end-diastole (IVSb) using long-axis images from a right-lateral recumbency view [29]. Apical 4 and 5 chamber images for Doppler measurements (velocity of transmitral flow during early and late diastole and their ratio [TMF; E wave, A wave, and E/A ratio], and that of a flow through LVOT, respectively) were obtained from a left lateral recumbency view. When EA fusion was seen, values of E and A waves of the cats were excluded from analysis (the same way as with STE and TDI).

Segmental thickness of the LV wall at the end-diastole was measured in the HCM group using LV short-axis images of the chordae tendineae level. The images used to measure LV wall thickness were the same as those used to analyze STE. The LV was divided into 6 regions (anteroseptum, anterior, lateral, posterior, inferior and septum), and those segments corresponded to the regions for the segmental strain and strain rate variables. The thickest region in each wall segment was measured.

Tissue Doppler echocardiography: The mitral annulus velocity (MAV) was measured at the lateral side in apical 4 chamber views. Peak values of MAV during systole and early diastole (Sa and Ea, respectively) were obtained, and E/Ea was derived from E wave divided by Ea.

Speckle tracking echocardiography: Right parasternal short-axis views at the Ct were used to measure all strain and strain rate variables. Images were acquired in cine loops triggered by the QRS complex, saved in a digital format and analyzed using off-line software (EchoPAC PC, GE Medical System, Tokyo, Japan). The principle behind speckle tracking analysis has been reported in several previous studies [4, 5, 18, 23, 24, 34–36, 39, 40]. The cardiac cycles used for analysis were determined by a simultaneous ECG (from R to R wave).

The peak systolic radial and circumferential strains (SR and SC), and the peak radial and circumferential strain rates during the systole and early diastole (SrRs, SrR_E, SrCs and SrC_E) were measured at the level of Ct (Fig. 1). The E/ SrR_E and E/ SrC_E were derived from E wave divided by SrR_E and SrC_E, respectively. All strain and strain rate variables were calculated by 6 segmental values (anteroseptum, anterior, lateral, posterior, inferior and septum). A global value was calculated as the mean value in all 6 segments.

In the present study, simultaneous ECG monitoring was not recorded in some cats with HCM, who were nervous and excited during an examination. Ideally, their images should be excluded from analysis. However, comparisons between STE variables that analyzed with simultaneous ECG monitoring and those without such monitoring showed good agreement (statistics analysis was performed using Bland-Altman plotting [Table 1 and Fig. 2]), and images unattached simultaneous ECG monitoring were allowed to include statistical analysis. In case images in the absence of simultaneous ECG monitoring were used for STE analysis, the frame at the time LV contracts the most right before LV distension was considered as proper timing of the end-diastole (R wave).

Study protocol: To determine the feasibility of radial and circumferential strain analysis using STE in the healthy cats, the following 4 factors were assessed: (1) percentage of LV wall segments capable of successfully analyzing strain and strain rate variables; (2) temporal resolution of images for STE analysis in cats; (3) influence of sedation; global strain and strain rate variables were obtained at the baseline and 15 min after sedation with acetylpromazine (0.01 mg/kg, SC) and buprenorphine (0.0075 mg/kg, SC) and then compared in 10 cats out of the healthy cats; and (4) inter- and intraobserver variabilities in offline analysis were also assessed in 6 healthy cats.

Then, global strain and strain rate variables in cats with HCM were compared with those in the healthy cats. Furthermore, segmental strain and strain rate variables were assessed for correlations with corresponding LV segmental

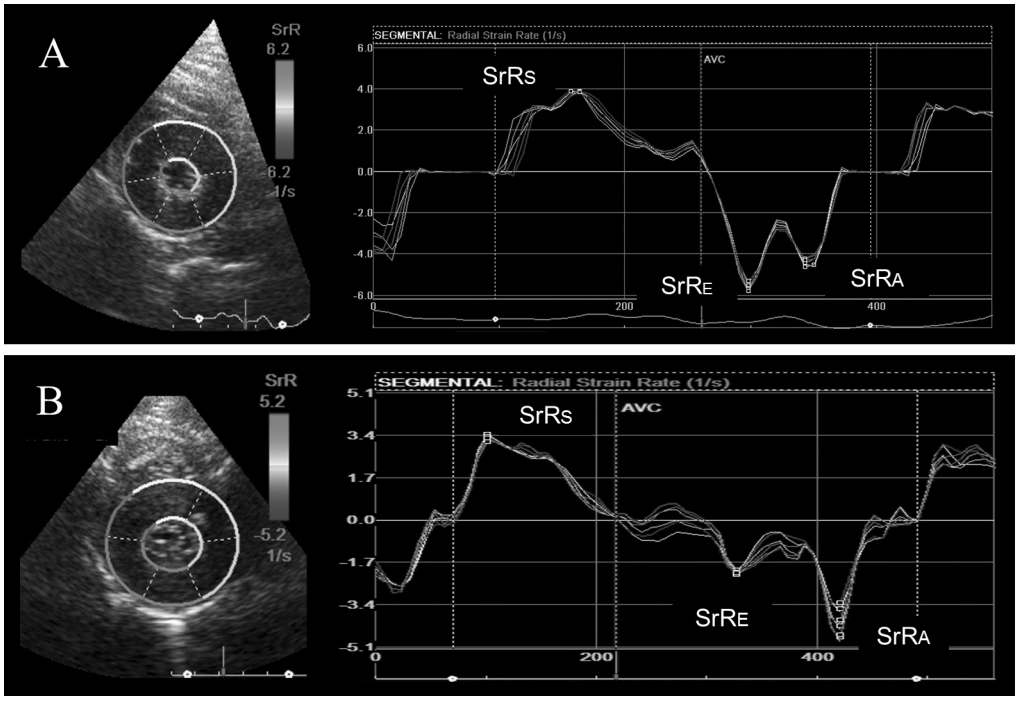

Fig. 1. Images of radial strain rate of a healthy cat (A) and a cat with hypertrophic cardiomyopathy (B). SrRs, radial strain rate during systole; SrR_E, radial strain rate during early diastole; SrR_A, radial strain rate during late diastole.

Table 1. Assessment of effects of STE variables with or without simultaneous ECG during analysis in healthy 10 cats

Parameter	Unit	Mean ± SD		Mean of the difference	Limits of agreement	r	*P* value
		With simultaneous ECG	Without simultaneous ECG				
SR	%	50.68 ± 8.05	52.11 ± 9.32	–1.53 ± 3.29	–8.00 to 5.14	0.94	<0.001
SrRs	/sec	3.79 ± 0.57	3.94 ± 0.70	–0.15 ± 0.41	–0.96 to 0.67	0.81	0.0041
SrR_E	/sec	–3.84 ± 1.19	–4.14 ± 1.16	0.29 ± 0.40	–0.51 to 1.10	0.94	<0.001
SC	%	–23.64 ± 3.75	–24.23 ± 4.76	0.59 ± 1.66	–2.73 to 3.91	0.95	<0.001
SrCs	/sec	–3.52 ± 0.46	–3.69 ± 0.53	0.17 ± 0.28	–0.39 to 0.73	0.85	0.0017
SrC_E	/sec	4.29 ± 1.32	4.44 ± 1.47	–0.15 ± 0.36	–0.87 to 0.57	0.97	<0.001

SD: standard deviation. r: coefficient of correlation. SR: peak systolic radial strain. SrRs: peak radial strain rate during systole. SrR_E: peak radial strain rate during early diastole. SC: peak systolic circumferential strain. SrCs: peak circumferential strain rate during systole. SrC_E: peak circumferential strain rate during early diastole.

hypertrophy.

Statistical analysis: Statistical analysis between the 2 groups was performed using a Student's or Welch's *t*-test when the data showed a normal distribution. When the normality test failed, a Mann-Whitney *U*-test was applied. One way ANOVA was applied for comparison of STE variables among the 6 segments of LV in the control groups. Assessment of the influence of sedation was performed using a paired *t*-test. When the normality test failed, a Wilcoxon signed-rank test was applied. For the comparisons between STE variables that analyzed with simultaneous ECG monitoring and those without such monitoring to assess agreement, Bland-Altman plotting was applied. Intra- and interobserver variability was expressed as a mean of the absolute difference as a percentage of the mean of two absolute measurements [24]. Multivariate regression analysis was applied to evaluate the relationships between STE variables and patient's conditions. The relationships between segmental STE variables and corresponding LV segmental wall thickness were determined by linear regression analysis. All parametric data were expressed as mean ± SD. Statistical significance was set at $P<0.05$.

RESULTS

The study population comprised the 16 healthy cats and the 17 cats with HCM. In the cats with HCM, atenolol (n=2), angiotensin-converting enzyme inhibitor (n=3) and thromboprophylaxis (n=2) were administered at the initial visit. One cat in the HCM group presented with congestive heart

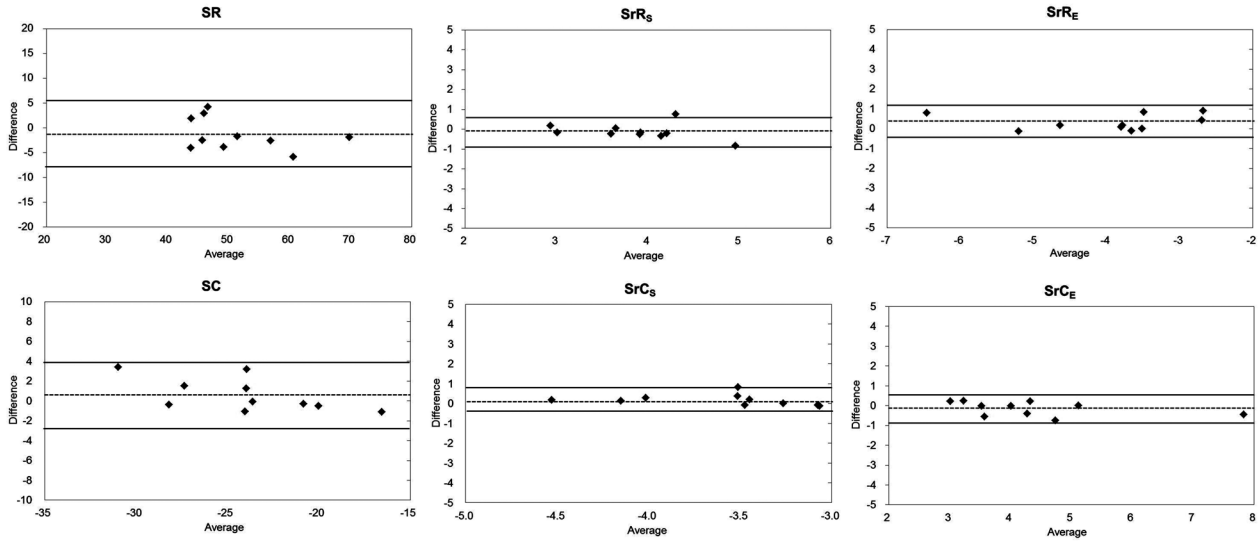

Fig. 2. Bland-Altman agreement plot comparing strain and strain rate variables analyzed with and without ECG monitoring in 10 healthy cats.

Table 2. Characteristics of healthy cats and cats with HCM

Parameter	Unit	Control Group		HCM Group		*P* value
Gender	F/M	F 8 / M 8	(16)	F 2 / M 15	(17)	–
BW	kg	4.14 ± 1.05	(16)	4.39 ± 1.00	(17)	0.49
Age	mo	40.56 ± 40.11	(16)	71.88 ± 50.24	(17)	<0.05
HR	bpm	182.75 ± 24.94	(16)	182.64 ± 43.58	(14)	0.99
SBP	mmHg	142.98 ± 10.15	(16)	125.88 ± 15.16	(11)	0.0017
USG	–	1.07 ± 0.02	(16)	1.04 ± 0.01	(6)	0.0011
BUN	mg/d*l*	27.94 ± 4.85	(16)	30.72 ± 17.53	(16)	>0.05
Cre	mg/d*l*	1.61 ± 0.36	(16)	1.85 ± 1.15	(16)	>0.05
IVSd	cm	0.38 ± 0.05	(16)	0.64 ± 0.11	(17)	<0.001
LVIDd	cm	1.49 ± 0.20	(16)	1.53 ± 0.22	(17)	>0.05
LVPWd	cm	0.40 ± 0.05	(16)	0.55 ± 0.16	(17)	0.0012
FS	%	42.71 ± 6.46	(16)	56.69 ± 7.87	(17)	<0.001
IVSb	cm	0.41 ± 0.06	(16)	0.70 ± 0.19	(16)	<0.001
LAD	cm	1.04 ± 0.13	(16)	1.39 ± 0.27	(16)	<0.001
LA/Ao	–	1.17 ± 0.09	(16)	1.36 ± 0.24	(15)	<0.05
E	cm/sec	67.45 ± 16.58	(16)	68.70 ± 22.68	(11)	0.87
A	cm/sec	58.53 ± 13.18	(16)	66.91 ± 26.99	(11)	0.36
E/A	–	1.19 ± 0.32	(16)	1.22 ± 0.78	(11)	>0.05
LVOTV	m/sec	0.96 ± 0.15	(16)	2.37 ± 1.51	(17)	0.0015
SAM	–	0 (0%)	(16)	5 (29%)	(17)	–
Sa	cm/sec	7.83 ± 2.33	(16)	6.17 ± 1.47	(8)	0.079
Ea	cm/sec	9.50 ± 2.67	(16)	6.76 ± 1.41	(7)	0.019
E/Ea	–	7.43 ± 2.19	(16)	10.28 ± 4.41	(5)	>0.05

BW: Body weight. HR: Heart rate. SBP: Systolic blood pressure. USG: Urine specific gravity. BUN: Blood urea nitrogen. Cre: Creatinine. IVSd: interventricular septum wall thickness at end-diastole. LVIDd: left ventricular end-diastolic internal diameter. LVPWd: left ventricular posterior wall thickness at end-diastole. FS: fractional shortening. IVSb: interventricular septum wall thickness above aortic valve at end-diastole. LA: left atrial diameter. LA/Ao: left atrium to aorta ratio. E: peak velocity of transmitral flow during early diastole. A: peak velocity of transmitral flow during late diastole. LVOTV: peak velocity of flow through left ventricular outflow tract. SAM: Systolic anterior motion of mitral valve. Sa: peak of mitral annulus velocity during systole. Ea: peak of mitral annulus velocity during early diastole.

Table 3. Global strain and strain rate variables in healthy cats and cats with HCM

Parameter		Unit	Control Group	HCM Group	*P* value
Radial	SR	%	47.13 ± 13.18 (16)	42.68 ± 17.29 (17)	0.41
	SrRs	/sec	3.57 ± 0.48 (16)	3.67 ± 1.08 (17)	0.74
	SrR_E	/sec	–3.69 ± 0.82 (16)	–2.59 ± 0.63 (8)	0.0030 a)
	E/SrR_E	–	–18.8 ± 5.27 (16)	–29.31 ± 9.07 (8)	0.0015 a)
Circumferential	SC	%	–24.38 ± 4.64 (16)	–23.15 ± 6.11 (17)	0.52
	SrCs	/sec	–3.43 ± 0.55 (16)	–3.57 ± 1.06 (17)	0.62
	SrC_E	/sec	4.52 ± 1.37 (13)	3.24 ± 0.78 (6)	0.049 a)
	E/SrC_E	–	16.4 ± 6.3 (13)	23.42 ± 6.06 (6)	0.035 a)

a) Significant difference, SR: peak systolic radial strain. SrRs: peak radial strain rate during systole. SrR_E: peak radial strain rate during early diastole. SC: peak systolic circumferential strain. SrCs: peak circumferential strain rate during systole. SrC_E: peak circumferential strain rate during early diastole.

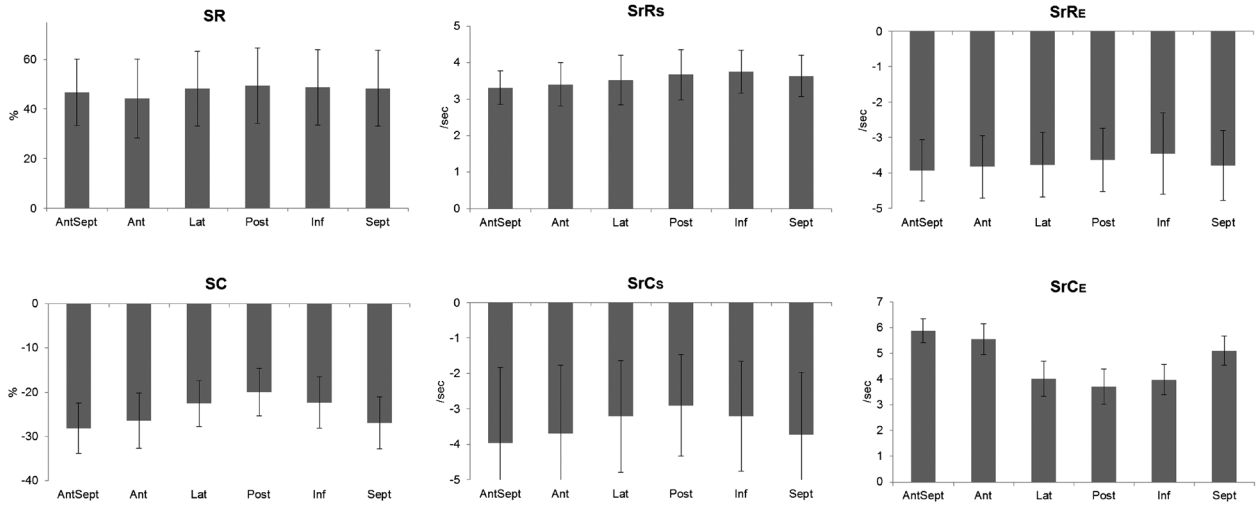

Fig. 3. Segmental strain and strain rate variables in left ventricular 6 segments of healthy cats.SR, radial strain; SrRs, radial strain rate during systole; SrR_E, radial strain rate during early diastole; SC, circumferential strain; SrCs, circumferential strain rate during systole; SrC_E, circumferential strain rate during early diastole.

failure, though others had no clinical sign. Seven cats exhibited a dynamic obstruction of LVOT. Although few cases had mitral regurgitation, they are judged as mild, because regions of their jet signals are limited. Only four cats had left atrial enlargement. The case characteristics and echocardiographic parameters are documented in Table 2.

Assessment of strain and strain rate variables using STE and feasibility of STE analysis in healthy cats: Results of global strain and strain rate variables in the healthy cats are shown in Table 3. In comparison of segmental variables among LV 6 segments, a significant difference was seen in all circumferential variables (SC; $P<0.001$, SrCS; $P<0.001$ and SrCE; $P=0.003$). However, no significant difference was seen in radial variables among the segments (SR; $P=0.93$, SrR_S; $P=0.27$ and SrR_E; $P=0.76$) (Fig. 3).

Ninety-seven point six percent of segments (281/288) were able to perform semi-auto tracking for an analysis of strain and strain rate variables. Although a fusion of E and A waves of SrR was not seen, one of SrC was observed in 3 cats out of the 16 healthy cats (18.8%).

The frame rate of acquired images used for STE analysis was 146.9 ± 13.1 fps (119–167 fps), and the rate per cardiac cycle (FPC) was 48.8 ± 5.9 frames.

Global strain and strain rate variables with and without sedation were compared (Table 4). No significant difference was seen between the 2 groups in any parameter. The intra- and inter-observer variability of each parameter is shown in Table 5.

Assessment of strain and strain rate variables in cats with HCM: Results of global strain and strain rate variables using STE in the cats with HCM are shown in Table 3. SrR_E, E/SrR_E, SrC_E and E/SrC_E exhibited significant differences between the healthy cats and those with HCM. However, multivariate regression analysis showed no significant relationships between STE variables and patient's condition, gender and age (Table 6). A fusion of E and A in SrR was observed in 9 cats and in SrC in 11, respectively, out of the 17 cats with HCM (52.9 and 64.7% each).

Measuring segmental LV wall thickness in HCM cats, patterns of LVH had variety. Relatively dominant hypertrophy

Table 4. Effect of sedation in healthy 10 cats

Parameter		Unit	Awake	Sedated	*P* value
Heart rate		bpm	180 ± 25	179 ± 19	0.44
Radial	SR	%	50.7 ± 8.05	44.7 ± 16.9	0.09
	SrRs	/sec	3.79 ± 0.57	3.85 ± 0.71	0.58
	SrR_E	/sec	–3.84 ± 1.19	–3.89 ± 0.84	0.88
Circumferential	SC	%	–23.6 ± 3.75	–23.3 ± 4.7	0.62
	SrCs	/sec	–3.24 ± 1.05	–3.71 ± 0.50	0.44
	SrC_E	/sec	4.29 ± 1.32	4.06 ± 0.99	0.19

SR: peak systolic radial strain. SrRs: peak radial strain rate during systole. SrR_E: peak radial strain rate during early diastole. SC: peak systolic circumferential strain. SrCs: peak circumferential strain rate during systole. SrC_E: peak circumferential strain rate during early diastole.

Table 5. Intra- and interobserver variability of each parameter in offline analysis

Parameter		Intraobserver (%)	Interobserver (%)
Radial	SR	5.54	8.45
	SrRs	4.1	8.09
	SrR_E	12.07	15.64
Circumferential	SC	4.93	5.56
	SrCs	6.75	4.75
	SrC_E	6.6	5.43

SR: peak systolic radial strain. SrRs: peak radial strain rate during systole. SrR_E: peak radial strain rate during early diastole. SC: peak systolic circumferential strain. SrCs: peak circumferential strain rate during systole. SrC_E: peak circumferential strain rate during early diastole.

in intraventricular wall and LV free wall was seen in 10 and 3 cats, respectively, out of the cats with HCM (59 and 18% each). Meanwhile, nearly homogeneous hypertrophy was seen in 4 cats out of the same (24%). Comparison of segmental strain and strain rate variables between LV wall segments with hypertrophy (thickness of LV wall during end-diastole is 6 mm or more) and those without hypertrophy (the same is less than 6 mm) in the cats with HCM revealed significant differences in SR and SrR_E (Table 7). However, no significant difference was observed in circumferential variables (Table 7). Segmental radial variables (SR and SrRs) and corresponding LV segmental wall thickness also showed significant relations, though their correlations were weak (SR, r=–0.23 *P*=0.018; SrRs, r=–0.20 *P*=0.047; and SrR_E, r=–0.20 *P*=0.062). No significant relation was observed in segmental circumferential variables (SC, r=–0.038 *P*=0.707; SrCs, r=–0.081 *P*=0.418; and SrC_E, r=–0.0017 *P*=0.987).

DISCUSSION

In the present study, we assessed the feasibility of analysis for radial and circumferential strain variables using STE in cats. Because of the relatively high heart rates of cats, it was anticipated that a somewhat inferior resolution in 2D images may have compromised the STE analysis. However, the STE proved both feasible and clinically acceptable in healthy cats. A high-frequency transducer allowed us to record an

Table 6. Multivariate regression analysis to evaluate relathionships between STE variables and patient's condition, gender and age

	Parameter	β	*P* value
SR	Patient's condition	–0.137	0.507
	Gender	0.109	0.577
	Age	–0.335	0.740
SrRS	Patient's condition	–0.018	0.930
	Gender	0.126	0.526
	Age	–0.038	0.846
SrR_E	Patient's condition	0.291	0.172
	Gender	0.007	0.970
	Age	0.234	0.239
SC	Patient's condition	0.109	0.597
	Gender	0.124	0.527
	Age	0.148	0.448
SrCS	Patient's condition	–0.088	0.669
	Gender	0.139	0.478
	Age	0.143	0.464
SrC_E	Patient's condition	–0.327	0.101
	Gender	–0.009	0.959
	Age	–0.17	0.358

SR: peak systolic radial strain. SrRs: peak radial strain rate during systole. SrR_E: peak radial strain rate during early diastole. SC: peak systolic circumferential strain. SrCs: peak circumferential strain rate during systole. SrC_E: peak circumferential strain rate during early diastole.

Table 7. Comparison of segmental radial strain and strain rate variables between left ventricular wall segments with and without hypertrophy in cats with HCM

Parameter		Unit	Non-hypertrophic segments		Hypertrophic segments		*P* value
Segmental LV wall thickness in diastole	Mean ± SD	mm	4.86 ± 0.59	(53)	6.86 ± 0.90	(49)	<0.001[a)]
	Range	mm	3.6–5.9	–	6.0–9.3	–	–
SR		%	47.27 ± 17.15	(53)	37.72 ± 17.68	(49)	0.007[a)]
SrRs		/sec	3.82 ± 1.13	(53)	3.51 ± 1.06	(49)	0.15
SrR_E		/sec	–3.34 ± 1.36	(41)	–2.68 ± 1.27	(44)	0.024[a)]
SC		%	–23.26 ± 8.54	(53)	–23.03 ± 6.89	(49)	0.88
SrCs		/sec	–3.69 ± 1.22	(53)	–3.45 ± 1.18	(49)	0.32
SrC_E		/sec	3.41 ± 1.44	(48)	3.49 ± 1.48	(45)	0.79

a): Significant difference, LV: left ventricle. SR: peak systolic radial strain. SrRs: peak radial strain rate during systole. SrR_E: peak radial strain rate during early diastole.

adequate quality of images and frame rates, even in cats with a small-sized heart. On the other hand, the FPC in cats appeared to be lower (48.8 ± 5.9 fpc) due to their high heart rates, when compared with those in dogs and humans (61.7 ± 20.9 [39] and 57-71fpc [42], respectively). Therefore, it might prove less accurate to assess STE parameters using time intervals in cats, compared with those in dogs and humans.

Furthermore, EA fusion due to their high heart rates would often interfere with assessment of diastolic function in cats, although it also posed even in TDI analysis and TMF measurements. In the present study, EA fusion was frequently exhibited in the circumferential strain rate rather than in the radial one. Keeping the cats as relaxed as possible or using sedatives to maintain low heart rate for them might help to diminish the prevalence of EA fusion when scanning an echocardiogram. It has been reported that decreased heart rate using drugs allows for assessment of E and A wave separately in cats [34].

The inter- and intraobserver variabilities of strain analysis in cats appeared to be satisfactory in the present study. Sedation with a combination of acepromazine and buprenorphine did not significantly influence strain and strain rate variables using STE in the present study. Since increased heart rates due to excitement during scanning may lead to a poor quality of images and EA fusion, sedation should be used as needed.

We evaluated whether or not it is possible to find significant difference of STE variables in cats with overt heart disease that may be detectable by morphological assessment using echocardiogram, in comparison with healthy cats. STE analysis in the present study could detect significant decrease of global radial and circumferential strain rate during early diastole in the cats with HCM, compared with healthy cats. In the present study, since almost cats with HCM did not have congestive heart failure and even left atrial enlargement, reduced global SrR_E and SrC_E may suggest the presence of impaired LV diastolic function due to LV hypertrophy and fibrosis in relatively early stage. However, since multivariate regression analysis did not show significant relationships between the STE variables and patient's condition, global STE variables in radial and circumferential directions could not detect impaired LV myocardial function.

Actually, in some studies in human patients with HCM, circumferential strain and strain variables have increased abnormally compared with controls in contrast to the studies described above and the present study [10, 15]. Values of circumferential strain also have been suggested to be different among layers of LV (epicardial, mid-myocardial and endocardial layers) in normal human subjects [3]. Furthermore, since endocardium is most susceptible to the deleterious effects of fibrosis and hypoperfusion [22], endocardial circumferential strain has been suggested to be able to identify regional ischemia accurately [19]. These factors may be one of the causes to occur the discrepancy in results of studies when circumferential strain is analyzed in a whole LV segment. Further assessments for circumferential strain and strain variables of the layers separately may be needed in cats. On the other hand, it has been suggested that circumferential strain variables increase or preserved appear to maintain to the normal LV ejection fraction as a compensation for longitudinal and radial strains [26, 42]. Because of different regional contributions of laminar mechanisms, regional systolic LV wall thickening is various. Sheet dynamics and sheet geometry of LV are important to systolic wall thickenings [11]. Further assessment of each change of strain variables in the 3 directions among different regions of LV in HCM of cats is needed.

In the present study, systolic indices of global STE variables including SR, SC, SrRs and SrCs did not decrease significantly in cats with HCM compared with controls. However, a significant decrease in longitudinal strain using TDI in cats with HCM has been previously reported [43]. Since it has been reported that LV myocardial contraction and relaxation were first impaired in the longitudinal direction among radial, circumferential and longitudinal ones in subclinical human patients with cardiovascular risk factors [26], longitudinal strain parameters might be sensitive enough to detect myocardial dysfunction in cats as well as humans. A further study to assess longitudinal deformation in cats will be necessary.

In the present study, a significant difference was seen in segmental radial strain and strain rate variables between hypertrophic and non-hypertrophic segments. Furthermore, segmental radial strain and strain rate variables had significant correlation with segmental LV thickness. It has been reported that LV segmental fibrosis and end-diastolic wall thickness were significantly related to segmental longitudinal strain in human patients with HCM [12, 33]. Assessing LV functions segmentally using STE, local ventricular dysfunctions could be detected even in the radial direction in the present study. This potentiality of STE may be useful in detections of left ventricular dysfunction in its early stage and asymmetric or local LVH with no concern for angle dependence. In addition, segmental values of strain and strain rate variables in radial direction are more invariant than those in circumferential direction among the LV 6 segments of normal subjects in the present study. The results of previous report using normal adults support the results of our present study [16]. This invariability may be useful to assess regional myocardial dysfunctions of LV.

This study had several limitations. First, diagnosis of LVH was based on morphological rather than pathological criteria. At the same time, we did not assess LV functions invasively, such as hemodynamic indices or severity of LV fibrosis, using MRI. Affected cats or LV segments may be included as normal and *vice versa*. Second, few cats with HCM were given medications, such as atenolol, at their examinations, and the fact that such medications may influence LV systolic and diastolic functions shall be taken into consideration [30, 41]. Third, in the present study, HCM cats with LVOTO were included in our analysis. HCM with LVOTO might have different LV systolic or diastolic myocardial functions compared with HCM which have no obstruction through LV outflow tract [10, 38]. Fourth, the male-female ratio was different between the control and HCM groups in the present study, because feline HCM is prevalent in male. LV func-

tions have been reported to have gender-specific change in human studies [28]. In healthy human adults, longitudinal and circumferential strains, except for a radial one, have showed a significant difference between genders [16]. Furthermore, a significant difference in age was also seen in the 2 groups of our study. Age-specific change in LV function also needs to be taken into consideration [28]. Longitudinal strain and strain rate have been reported to decrease significantly in an older population compared with a young one in a human study, though no significant difference was seen in the radial and circumferential strain and strain rate in systole and early diastole [32]. Further studies to assess gender- and age-specific differences in strain and strain rate variables using STE are warranted even in cats.

In conclusion, radial and circumferential strain analysis using STE was considered clinically feasible for assessing cardiac functions in cats. In LV segments of cats with HCM, reduced segmental radial strain and strain rate variables have possibility to have relations with LV segmental hypertrophy. In short axis image of LV in cats with HCM, radial strain and strain rate variables have possibility to detect myocardial dysfunctions locally and early. Further studies are warranted to demonstrate clinical availability of STE in cats.

REFERENCES

1. Abbott, J. A. 2010. Feline hypertrophic cardiomyopathy: an update. *Vet. Clin. North Am. Small Anim. Pract.* **40**: 685–700. [Medline] [CrossRef]
2. Abbott, J. A. and MacLean, H. N. 2006. Two-dimensional echocardiographic assessment of the feline left atrium. *J. Vet. Intern. Med.* **20**: 111–119. [Medline] [CrossRef]
3. Adamu, U., Schmitz, F., Becker, M., Kelm, M. and Hoffmann, R. 2009. Advanced speckle tracking echocardiography allowing a three-myocardial layer-specific analysis of deformation parameters. *Eur. J. Echocardiogr.* **10**: 303–308. [Medline] [CrossRef]
4. Amundsen, B. H., Helle-Valle, T., Edvardsen, T., Torp, H., Crosby, J., Lyseggen, E., Støylen, A., Ihlen, H., Lima, J. A., Smiseth, O. A. and Slørdahl, S. A. 2006. Noninvasive myocardial strain measurement by speckle tracking echocardiography: validation against sonomicrometry and tagged magnetic resonance imaging. *J. Am. Coll. Cardiol.* **47**: 789–793. [Medline] [CrossRef]
5. Becker, M., Bilke, E., Kühl, H., Katoh, M., Kramann, R., Franke, A., Bücker, A., Hanrath, P. and Hoffmann, R. 2006. Analysis of myocardial deformation based on pixel tracking in two dimensional echocardiographic images enables quantitative assessment of regional left ventricular function. *Heart* **92**: 1102–1108. [Medline] [CrossRef]
6. Bond, B. R., Fox, P. R., Peterson, M. E. and Skavaril, R. V. 1988. Echocardiographic findings in 103 cats with hyperthyroidism. *J. Am. Vet. Med. Assoc.* **192**: 1546–1549. [Medline]
7. Brizard, D., Amberger, C., Hartnack, S., Doherr, M. and Lombard, C. 2009. Phenotypes and echocardiographic characteristics of a European population of domestic shorthair cats with idiopathic hypertrophic cardiomyopathy. *Schweiz. Arch. Tierheilkd.* **151**: 529–538. [Medline] [CrossRef]
8. Broussard, J. D., Peterson, M. E. and Fox, P. R. 1995. Changes in clinical and laboratory findings in cats with hyperthyroidism from 1983 to 1993. *J. Am. Vet. Med. Assoc.* **206**: 302–305. [Medline]
9. Brown, S., Atkins, C., Bagley, R., Carr, A., Cowgill, L., Davidson, M., Egner, B., Elliott, J., Henik, R., Labato, M., Littman, M., Polzin, D., Ross, L., Snyder, P., Stepien R., American College of Veterinary Internal Medicine 2007. Guidelines for the identification, evaluation, and management of systemic hypertension in dogs and cats. *J. Vet. Intern. Med.* **21**: 542–558. [Medline] [CrossRef]
10. Carasso, S., Yang, H., Woo, A., Vannan, M. A., Jamorski, M., Wigle, E. D. and Rakowski, H. 2008. Systolic myocardial mechanics in hypertrophic cardiomyopathy: novel concepts and implications for clinical status. *J. Am. Soc. Echocardiogr.* **21**: 675–683. [Medline] [CrossRef]
11. Cheng, A., Nguyen, T. C., Malinowski, M., Daughters, G. T., Miller, D. C. and Ingels, N. B. Jr. 2008. Heterogeneity of left ventricular wall thickening mechanisms. *Circulation* **118**: 713–721. [Medline] [CrossRef]
12. Chang, S. A., Lee, S. C., Choe, Y. H., Hahn, H. J., Jang, S. Y., Park, S. J., Choi, J. O., Park, S. W. and Oh, J. K. 2012. Effects of hypertrophy and fibrosis on regional and global functional heterogeneity in hypertrophic cardiomyopathy. *Int. J. Cardiovasc. Imaging* **28** Suppl 2: 133–140. [Medline] [CrossRef]
13. Chetboul, V., Lefebvre, H. P., Pinhas, C., Clerc, B., Boussouf, M. and Pouchelon, J. L. 2003. Spontaneous feline hypertension: clinical and echocardiographic abnormalities, and survival rate. *J. Vet. Intern. Med.* **17**: 89–95. [Medline] [CrossRef]
14. Edvardsen, T., Helle-Valle, T. and Smiseth, O. A. 2006. Systolic dysfunction in heart failure with normal ejection fraction: speckle-tracking echocardiography. *Prog. Cardiovasc. Dis.* **49**: 207–214. [Medline] [CrossRef]
15. Garceau, P., Carasso, S., Woo, A., Overgaard, C., Schwartz, L. and Rakowski, H. 2012. Evaluation of left ventricular relaxation and filling pressures in obstructive hypertrophic cardiomyopathy: comparison between invasive hemodynamics and two-dimensional speckle tracking. *Echocardiography* **29**: 934–942. [Medline] [CrossRef]
16. Hurlburt, H. M., Aurigemma, G. P., Hill, J. C., Narayanan, A., Gaasch, W. H., Vinch, C. S., Meyer, T. E. and Tighe, D. A. 2007. Direct ultrasound measurement of longitudinal, circumferential, and radial strain using 2-dimensional strain imaging in normal adults. *Echocardiography* **24**: 723–731. [Medline] [CrossRef]
17. Hurty, C. A. and Flatland, B. 2005. Feline acromegaly: a review of the syndrome. *J. Am. Anim. Hosp. Assoc.* **41**: 292–297. [Medline] [CrossRef]
18. Kim, H. K., Sohn, D. W., Lee, S. E., Choi, S. Y., Park, J. S., Kim, Y. J., Oh, B. H., Park, Y. B. and Choi, Y. S. 2007. Assessment of left ventricular rotation and torsion with two-dimensional speckle tracking echocardiography. *J. Am. Soc. Echocardiogr.* **20**: 45–53. [Medline] [CrossRef]
19. Kimura, K., Takenaka, K., Ebihara, A., Uno, K., Iwata, H., Sata, M., Kohro, T., Morita, H., Yatomi, Y. and Nagai, R. 2011. Reproducibility and diagnostic accuracy of three-layer speckle tracking echocardiography in a swine chronic ischemia model. *Echocardiography* **28**: 1148–1155. [Medline] [CrossRef]
20. Koffas, H., Dukes-McEwan, J., Corcoran, B. M., Moran, C. M., French, A., Sboros, V., Simpson, K. and McDicken, W. N. 2006. Pulsed tissue Doppler imaging in normal cats and cats with hypertrophic cardiomyopathy. *J. Vet. Intern. Med.* **20**: 65–77. [Medline] [CrossRef]
21. MacDonald, K. A., Kittleson, M. D., Garcia-Nolen, T., Larson, R. F. and Wisner, E. R. 2006. Tissue Doppler imaging and gradient echo cardiac magnetic resonance imaging in normal cats and cats with hypertrophic cardiomyopathy. *J. Vet. Intern. Med.* **20**: 627–634. [Medline] [CrossRef]

22. Martinez, D. A., Guhl, D. J., Stanley, W. C. and Vailas, A. C. 2003. Extracellular matrix maturation in the left ventricle of normal and diabetic swine. *Diabetes Res. Clin. Pract.* **59**: 1–9. [Medline] [CrossRef]
23. Meluzin, J., Spinarova, L., Hude, P., Krejci, J., Podrouzkova, H., Pesl, M., Orban, M., Dusek, L., Jarkovsky, J. and Korinek, J. 2011. Estimation of left ventricular filling pressures by speckle tracking echocardiography in patients with idiopathic dilated cardiomyopathy. *Eur. J. Echocardiogr.* **12**: 11–18. [Medline] [CrossRef]
24. Meluzin, J., Spinarova, L., Hude, P., Krejci, J., Poloczkova, H., Podrouzkova, H., Pesl, M., Orban, M., Dusek, L. and Korinek, J. 2009. Left ventricular mechanics in idiopathic dilated cardiomyopathy: systolic-diastolic coupling and torsion. *J. Am. Soc. Echocardiogr.* **22**: 486–493. [Medline] [CrossRef]
25. Milner, R. J., Channell, C. D., Levy, J. K. and Schaer, M. 2006. Survival times for cats with hyperthyroidism treated with iodine 131, methimazole, or both: 167 cases (1996–2003). *J. Am. Vet. Med. Assoc.* **228**: 559–563. [Medline] [CrossRef]
26. Mizuguchi, Y., Oishi, Y., Miyoshi, H., Iuchi, A., Nagase, N. and Oki, T. 2008. The functional role of longitudinal, circumferential, and radial myocardial deformation for regulating the early impairment of left ventricular contraction and relaxation in patients with cardiovascular risk factors: a study with two-dimensional strain imaging. *J. Am. Soc. Echocardiogr.* **21**: 1138–1144. [Medline] [CrossRef]
27. Nishimura, R. A. and Holmes, D. R. Jr. 2004. Clinical practice. Hypertrophic obstructive cardiomyopathy. *N. Engl. J. Med.* **350**: 1320–1327. [Medline] [CrossRef]
28. Okura, H., Takada, Y., Yamabe, A., Kubo, T., Asawa, K., Ozaki, T., Yamagishi, H., Toda, I., Yoshiyama, M., Yoshikawa, J. and Yoshida, K. 2009. Age- and gender-specific changes in the left ventricular relaxation: a Doppler echocardiographic study in healthy individuals. *Circ. Cardiovasc. Imaging* **2**: 41–46. [Medline] [CrossRef]
29. Paige, C. F., Abbott, J. A., Elvinger, F. and Pyle, R. L. 2009. Prevalence of cardiomyopathy in apparently healthy cats. *J. Am. Vet. Med. Assoc.* **234**: 1398–1403. [Medline] [CrossRef]
30. Palmieri, V., Russo, C., Palmieri, E. A., Pezzullo, S. and Celentano, A. 2009. Changes in components of left ventricular mechanics under selective beta-1 blockade: insight from traditional and new technologies in echocardiography. *Eur. J. Echocardiogr.* **10**: 745–752. [Medline] [CrossRef]
31. Peterson, M. E., Taylor, R. S., Greco, D. S., Nelson, R. W., Randolph, J. F., Foodman, M. S., Moroff, S. D., Morrison, S. A. and Lothrop, C. D. 1990. Acromegaly in 14 cats. *J. Vet. Intern. Med.* **4**: 192–201. [Medline] [CrossRef]
32. Phan, T. T., Shivu, G. N., Abozguia, K., Gnanadevan, M., Ahmed, I. and Frenneaux, M. 2009. Left ventricular torsion and strain patterns in heart failure with normal ejection fraction are similar to age-related changes. *Eur. J. Echocardiogr.* **10**: 793–800. [Medline] [CrossRef]
33. Popović, Z. B., Kwon, D. H., Mishra, M., Buakhamsri, A., Greenberg, N. L., Thamilarasan, M., Flamm, S. D., Thomas, J. D., Lever, H. M. and Desai, M. Y. 2008. Association between regional ventricular function and myocardial fibrosis in hypertrophic cardiomyopathy assessed by speckle tracking echocardiography and delayed hyperenhancement magnetic resonance imaging. *J. Am. Soc. Echocardiogr.* **21**: 1299–1305. [Medline] [CrossRef]
34. Riesen, S. C., Schober, K. E., Cervenec, R. M. and Bonagura, J. D. 2011. Comparison of the effects of ivabradine and atenolol on heart rate and echocardiographic variables of left heart function in healthy cats. *J. Vet. Intern. Med.* **25**: 469–476. [Medline] [CrossRef]
35. Riesen, S. C., Schober, K. E., Cervenec, R. M. and Bonagura, J. D. 2012. Effects of treatment with ivabradine and atenolol on reproducibility of echocardiographic indices of left heart size and function in healthy cats. *J. Vet. Cardiol.* **14**: 323–332. [Medline] [CrossRef]
36. Riesen, S. C., Schober, K. E., Smith, D. N., Otoni, C. C., Li, X. and Bonagura, J. D. 2012. Effects of ivabradine on heart rate and left ventricular function in healthy cats and cats with hypertrophic cardiomyopathy. *Am. J. Vet. Res.* **73**: 202–212. [Medline] [CrossRef]
37. Serri, K., Reant, P., Lafitte, M., Berhouet, M., Le Bouffos, V., Roudaut, R. and Lafitte, S. 2006. Global and regional myocardial function quantification by two-dimensional strain: application in hypertrophic cardiomyopathy. *J. Am. Coll. Cardiol.* **47**: 1175–1181. [Medline] [CrossRef]
38. Simpson, K. E., Gunn-Moore, D. A., Shaw, D. J., French, A. T., Dukes-McEwan, J., Moran, C. M. and Corcoran, B. M. 2009. Pulsed-wave Doppler tissue imaging velocities in normal geriatric cats and geriatric cats with primary or systemic diseases linked to specific cardiomyopathies in humans, and the influence of age and heart rate upon these velocities. *J. Feline Med. Surg.* **11**: 293–304. [Medline] [CrossRef]
39. Takano, H., Fujii, Y., Ishikawa, R., Aoki, T. and Wakao, Y. 2010. Comparison of left ventricular contraction profiles among small, medium, and large dogs by use of two-dimensional speckle-tracking echocardiography. *Am. J. Vet. Res.* **71**: 421–427. [Medline] [CrossRef]
40. Takano, H., Fujii, Y., Yugeta, N., Takeda, S. and Wakao, Y. 2011. Assessment of left ventricular regional function in affected and carrier dogs with Duchenne muscular dystrophy using speckle tracking echocardiography. *BMC Cardiovasc. Disord.* **11**: 23. [Medline]
41. Tapp, R. J., Sharp, A., Stanton, A. V., O'Brien, E., Chaturvedi, N., Poulter, N. R., Sever, P. S., Thom, S. A., Hughes, A. D., Mayet, J., ASCOT Investigators 2010. Differential effects of antihypertensive treatment on left ventricular diastolic function: an ASCOT (Anglo-Scandinavian Cardiac Outcomes Trial) substudy. *J. Am. Coll. Cardiol.* **55**: 1875–1881. [Medline] [CrossRef]
42. Wang, J., Khoury, D. S., Yue, Y., Torre-Amione, G. and Nagueh, S. F. 2008. Preserved left ventricular twist and circumferential deformation, but depressed longitudinal and radial deformation in patients with diastolic heart failure. *Eur. Heart J.* **29**: 1283–1289. [Medline] [CrossRef]
43. Wess, G., Sarkar, R. and Hartmann, K. 2010. Assessment of left ventricular systolic function by strain imaging echocardiography in various stages of feline hypertrophic cardiomyopathy. *J. Vet. Intern. Med.* **24**: 1375–1382. [Medline] [CrossRef]